Available online at www.sciencedirect.com
SCIENCE DIRECT®
Applied Surface Science 248 (2005) 62–65
applied surface science
www.elsevier.com/locate/apsusc

Study of hot-carrier-induced photon emission from 90 nm Si MOSFETs

M. Gurfinkel [a,*], M. Borenshtein [b], A. Margulis [b], S. Sade [b], Y. Fefer [b], Y. Weizman [b], Yoram Shapira [a]

[a] *School of Electrical Engineering, Tel-Aviv University, Ramat-Aviv 69978, Israel*
[b] *Freescale Semiconductor Israel Ltd., Herzlia 46725, Israel*

Available online 18 March 2005

Abstract

Measurements of photon emission and substrate current in metal-oxide-semiconductor field effect transistors at various temperatures have been carried out using electrical and NIR microscopy. The results received at room temperature have extended the correlation between the substrate current and the photon emission, which was previously found in the visible, to the NIR range. On the basis of this correlation, an empirical model based on the substrate current was used to describe the static emission intensity dependence on the transistor bias. Temperature resolved measurements show that the correlation between emission intensity and the substrate current appears to be coincidental.

PACS: 85.30.Tv; 85.40.Qx; 78.60.Fi

Keywords: MOSFET; Hot carrier luminescence; Photon emission; Substrate current; Semiconductor device models

1. Introduction

The exponential increase in the density, complexity and speed of ULSI circuits makes the task of testing them increasingly difficult. Photon emission, induced by hot carriers in metal-oxide-semiconductor field effect transistors (MOSFETs) operating in the saturation region, has been the most direct means to probe hot-carrier phenomena in complementary metal-oxide-semiconductor (CMOS) circuits. Historically, reliability was the primary concern and trigger that generated extensive studies of hot carrier emission [1–4]. The emission intensity and spectra have been suggested for device lifetime monitoring since it is known that photon emission, like other hot-electron effects, is driven by the channel electric field [5].

In recent years, renewed interest in the issue is emerging due to the possibility to exploit the emission for circuit debugging and analysis. Since the transistors in CMOS circuits unavoidably cross the saturation region, photons which are generated during

* Corresponding author. Fax: +972 3 6423508.
E-mail address: moshegur@post.tau.ac.il (M. Gurfinkel).

0169-4332/$ – see front matter
doi:10.1016/j.apsusc.2005.03.033

normal device operation, can serve as indicators for logic transitions in time-resolved inspection [6]. Thus, photon emission is becoming a useful technique for non-invasive probing in the <0.1 μm era. In spite of the intensive research in the past three decades, the physical mechanism behind photon emission is still controversial. Several theories have been proposed to explain photon emission. Because of the Si indirect band structure, radiative electron–hole recombination may occur only through phonon-assisted or impurity-induced processes. These band-to-band recombination processes are so inefficient in silicon that other luminescent processes, although producing very little light, may become significant. Of special interest is hot-carrier emission by intraband transitions and bremsstrahlung [7].

The correlation between the substrate current, I_{sub}, originating from impact ionization of hot electrons under the high electrical field near the drain, and the hot-carrier-induced photon emission is well established [8,9]. The two phenomena are both hot carrier effects driven by the channel electric field, or more specifically, at the maximum channel electric field, E_m, which exists at the channel drain end.

Since all hot-electron effects are correlated, device lifetime can be monitored using any hot-electron mechanism, but until now, I_{sub} is regarded the best lifetime monitor. Using measurements of static emission intensity under various electrical and physical conditions of the transistor, we demonstrate that the correlation between the substrate current and emission intensity is valid only if we ignore the temperature dependence. An empirical model describing the static emission intensity is reported.

2. Experimental details

Static emission and electrical measurements were taken on a test device that was manufactured using a 90 nm advanced microprocessor technology. The device used for measurements was *n*-MOSFET with a gate length of 0.08 μm and a transistor width of 9.69 μm. *I–V* characteristics and substrate currents were measured using a semiconductor parameter analyzer model HP4155B. The device emission characteristics were evaluated using an IR emission cryogenically cooled MgCdTe CCD microscope with spectral response ranging between 800 and 1500 nm. The total emission intensity is integrated over the entire spectral response of the detector and summed for all pixel values that correspond to the transistor region.

3. Results and discussion

Fig. 1 shows the emission intensity from an *n*-channel MOS transistor as a function of the gate-source voltage, V_{gs} for several drain-source voltages, V_{ds} (V_{ds} = 1.3 V (triangles), V_{ds} = 1.2 V (diamonds) and V_{ds} = 1.1 V (squares)). The curves are calculated on the basis of the theoretical model described in the following section.

Fig. 2 shows the emission intensity and substrate current I_{sub}, both normalized to their maximum value, as a function of V_{gs} at V_{ds} = 1.3 V. The circles represent the measured emission values, the squares represent the measured substrate current values, and the solid curve represents the theoretical model used.

Many authors have demonstrated a correlation between the substrate current I_{sub} and the emission intensity at the high energy (visible) photon tail [8–10]. Our measurements (see Fig. 2) show that this correlation may be extended into the near IR range, in which the photon emission rate is 1–2 orders of magnitude higher than in the visible.

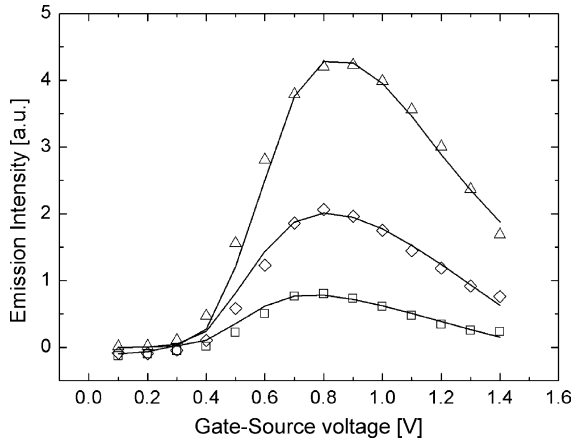

Fig. 1. Total emission intensity as a function of V_{gs} for different V_{ds} voltages. Triangles: V_{ds} = 1.3 V, diamonds: V_{ds} = 1.2 V, squares: V_{ds} = 1.1 V and solid curves: from the theoretical model.

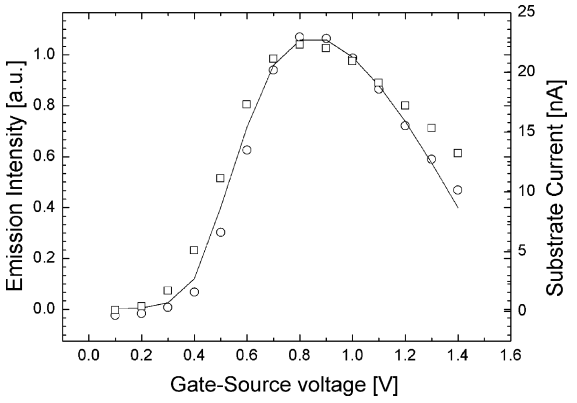

Fig. 2. Total emission intensity and substrate current (both normalized to their maximum value) as a function of V_{gs} at V_{ds} = 1.3 V. The circles represent the measured emission values, squares represent the measured substrate current, and the solid curve represents the theoretical model.

According to this correlation we may use a substrate–current-based theoretical model to describe the emission intensity. We use the substrate current model based on Li et al. [11]:

$$I_{sub} = C_1 I_D E_m \ell_d \, e^{-B_i/E_m} \quad (1)$$

where I_D is the channel current, E_m the maximum electrical field in the channel, ℓ_d is the characteristic length of the velocity saturation region, B_i is the impact ionization constant (where the impact ionization coefficient is defined as $\alpha = A_i \, e^{-B_i/E}$, E is the electric field) and C_1 is a proportionality coefficient. We can approximate the maximum electric field by $E_m \approx (V_{ds} - V_{ds,sat})/\ell_d$ [5], where $V_{ds,sat}$ is the drain-source voltage at which carrier velocity saturates. Thus, the equation for the substrate current is

$$I_{sub} = C_1 I_D (V_{ds} - V_{ds,sat}) \, e^{-B_i \ell_d/(V_d - V_{ds,sat})} \quad (2)$$

The similarity in the appearance of the emission intensity and substrate current behaviors has been attributed to the similar field dependence of both phenomena. We use this similarity to apply the substrate current model to the emission study.

By replacing the impact ionization constant B_i with a photoemission rate constant B_{PH} we get

$$N_{PH} = A_1 I_D (V_{ds} - V_{ds,sat}) \, e^{-B_{PH} \ell_d/(V_d - V_{ds,sat})} \quad (3)$$

where N_{PH} is the photon emission intensity.

Since the classical dependence $V_{ds,sat} = V_{gs} - V_{th}$ is not valid for short channel devices, the value of $V_{ds,sat}$ is taken from the BSIM3V3.2.2 short channel MOSFET model [12] as

$$V_{ds,sat} = \frac{E_{sat} L (V_{gs} - V_{th} + 2V_t)}{E_{sat} L + V_{gs} - V_{th} + 2V_t} \quad (4)$$

where L is the channel length, V_g the gate bias, V_{th} the threshold voltage, E_{sat} the channel electric field at which the carriers reach the velocity saturation, and V_t the thermal voltage.

The theoretical model given by Eq. (3) shows a very good agreement with the measured emission intensity as shown in Fig. 1.

ℓ_d is a function of the process parameters and is also affected by E_m [11]. A first order approximation is $\ell_d \approx \sqrt{\varepsilon_{Si} t_{ox} X_j / \varepsilon_{ox}}$, where t_{ox} is the gate-oxide thickness, X_j the drain junction depth, and ε_{Si} and ε_{ox} are the dielectric permittivities of Si and SiO_2, respectively. By using the corrected, field dependent values of ℓ_d (from Li et al. [11]), the fitting was improved by approximately 5%, as shown in Fig. 1.

The parameters A_1 and B_{PH}, in Eq. (3), are extracted by fitting the model to the measured data.

The measured substrate current at room temperature shows a close correlation to the shape of the total emission, both experimentally and theoretically, as seen in Fig. 2. The difference between the photon emission intensity and substrate current values is a function of the detector spectral range [4].

By fitting the measured emission intensity to the photoemission model and extracting the emission rate constant we get $B_{PH} = (5.3 \pm 0.2) \times 10^6$ V/cm. In a similar manner we extract the impact ionization constant from the substrate current measurements and obtain $B_i = (5.7 \pm 0.2) \times 10^6$ V/cm. The similarity between the two rate constants does not imply that their physical mechanism is identical.

Fig. 3 shows the emission intensity (a) and the substrate current (b) measured as a function of V_{gs} at a fixed V_{ds} for three different temperatures (296 K (squares), 325 K (circles) and 363 K (triangles)). The results show that the emission intensity dependence on the temperature in this range is negligible. The minor deviations in emission intensity as a function of temperature are attributed to changes in the channel current and are eliminated by normalizing the results to I_{ds}.

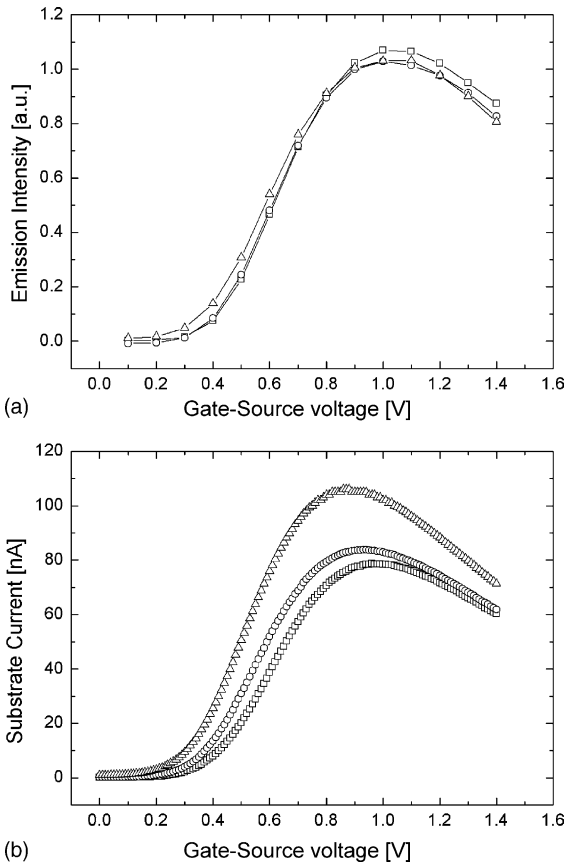

Fig. 3. (a) The emission intensity at different temperatures as a function of V_{gs} at $V_{ds} = 1.4$ V; (b) substrate current at different temperatures as function of V_{gs} at $V_{ds} = 1.4$ V. Squares: $T = 296$ K, circles: $T = 325$ K and triangles: $T = 363$ K.

Fig. 3a shows that the photoemission rate constant B_{PH} does not depend on the lattice temperature in the range of 296–363 K. We note that $V_{ds,sat}$ and thus E_m must be temperature dependent but this dependence is quite small [13]. However, the impact ionization rate and the impact ionization constant B_i are clearly dependent on the lattice temperature. Eitan et al. [14] have shown that in MOSFETs the impact ionization rate decreases with temperature for high drain biases ($V_{ds} > 1.75$ V) and increases with temperature for low drain biases ($V_{ds} < 1.75$ V). In our case ($V_{ds} = 1.4$ V), the impact ionization rate and consequently the substrate current increase significantly with temperature (Fig. 3b). The different temperature dependence of the photon emission intensity and the substrate current suggests that their physical mechanisms are different. The correlation between the two phenomena appears to be coincidental, as suggested by Tam and Hu [8], and applies only to a specific temperature.

4. Conclusions

Measurements from 90 nm MOSFETs at room temperature have extended the correlation between the substrate current and the photon emission, which was previously found in the visible range, to the NIR range. An empirical model describing the static emission intensity dependence on transistor bias is reported. Temperature resolved measurements show different temperature dependences for the photon emission and the substrate current.

References

[1] Y. Uraoka, N. Tsutsu, Y. Nakata, S. Akiyama, IEEE Trans. Semicond. Manuf. 4 (1991) 183.
[2] L. Selmi, Microelectron. Eng. 28 (1995) 249.
[3] L. Selmi, M. Pavesi, H.S.P. Wong, A. Acovic, E. Sangiorgi, IEEE Trans. Electron Dev. 45 (1998) 1135.
[4] N. Tsutsu, Y. Uraoka, Y. Nakata, S. Akiyama, H. Esaki, in: Proceedings of the International Conference on Microelectronic Test Structures, IEEE-ICMTS, 1990, , pp. 143–148.
[5] C. Hu, S.C. Tam, F.C. Hsu, P.K. Ko, T.Y. Chan, K.W. Terrill, IEEE Trans. Electron Dev. 32 (1985) 375.
[6] J.C. Tsang, J.A. Kash, D.P. Vallett, IBM J. Res. Develop. 44 (2000) 583.
[7] J. Bude, N. Sano, A. Yoshii, Phys. Rev. B 45 (1992) 5848.
[8] S. Tam, C. Hu, IEEE Trans. Electron Dev. 31 (1984) 1264.
[9] P.A. Childs, R.A. Stuart, W. Eccleston, Solid-State Electron. 26 (1983) 685.
[10] A. Toriumi, M. Yoshimi, M. Iwase, Y. Akiyama, K. Taniguchi, IEEE Trans. Electron Dev. 34 (1987) 1502.
[11] W. Li, J.S. Yuan, S. Chetlur, J. Zhou, A.S. Oates, Solid-State Electron. 44 (2000) 1985.
[12] W. Liu, X. Jin, J. Chen, M. Jeng, Z. Liu, Y. Cheng, K. Chen, M. Chan, K. Hui, J. Huang, R. Tu, P. Ko, C. Hu, BSIM3V3.2.2 MOSFET Model, Users' Manual, 1999.
[13] N.D. Arora, M.S. Sharma, IEEE Trans. Electron Dev. 38 (1991) 1392.
[14] B. Eitan, C. Frohman-Bentchkowsky, J. Shapir, J. Appl. Phys. 53 (1982) 1244.